

# Performance of Distillation Protocols under EPR Pair Initialization and Gate Errors

Matteo Arfini (5497523), Daniel Bedialauneta Rodríguez (5567025),  
Marc Serra Peralta (5623510) and Ksenia Shagalov (5474574)

## ABSTRACT

Sharing maximally entangled pairs is essential in quantum information processing, but the unwanted interactions with the environment limit the entanglement fidelity of the produced pairs. A method to overcome such problem is entanglement distillation, whose aim is to create higher-fidelity entangled pairs from a larger number of lower-fidelity pairs. In this report, we analyse the performance of BBPSSW, DEJMPS, 3-to-1 (described in [1]) and EPL protocols for entanglement distillation when using Werner states and imperfect gates. In particular, this report is focused on the dependence of the increase of fidelity with respect to the input pair and gate fidelities. The results are obtained by numerical simulation using the NetSquid simulator. Upon the characterization of the numerical errors, we show that all four protocols display an increase in the pair fidelity for a gate fidelity higher than  $\sim 0.96$  and that the higher the success fidelity, the lower success probability, as predicted theoretically. Moreover, we build a simple recipe to select the most useful protocol given a list of requirements and hardware performance. The results obtained in the simulations highlight the practical limitations of entanglement distillation protocols and reflect the necessity for further investigation. These include a theoretical model for the EPL protocol implemented with Werner states, the addition of noisy measurements in the simulated protocols and the increase in the number of simulations to achieve higher accuracy.

## I. INTRODUCTION

Entanglement is an essential resource in quantum information and communication because it is consumed as form of EPR pairs by many protocols, such as quantum teleportation, superdense coding and entanglement-based quantum cryptography [2]. Therefore, the distribution of pure maximally entangled states over distant locations is required for the large-scale realization of quantum communication schemes. In a real scenario, environmental noise or imperfect gate operations reduce both purity and entanglement of a given EPR pair, leading to a fidelity with respect to the perfect target state ( $F$ ) smaller than one.

A way to model the pair initialization noise and imperfect gates is through a depolarising channel, which returns the original state with probability  $p$  and the maximally mixed state with probability  $1 - p$  [3]. Then, the noisy EPR state shared between two parties is in the form of a Werner state

$$\rho(p) = p |\phi_{00}\rangle \langle \phi_{00}| + \frac{1-p}{4} \mathbb{1} \quad (1)$$

where  $|\phi_{00}\rangle = (|00\rangle + |11\rangle)/\sqrt{2}$  and  $p$  is the parameter of the depolarizing channel. The fidelity of such state with respect to  $|\phi_{00}\rangle$  is related to  $p$  by  $F = (1 + 3p)/4$ .

In order to achieve higher fidelity pairs, one can apply entanglement distillation. These protocols start from  $N$  noisy

EPR pairs to create  $M < N$  pairs with higher entanglement and higher degree of purity by using so-called local operations and classical communication [2]. The successful outcome of entanglement distillation protocols is evaluated by means of the output fidelity with respect to  $|\phi_{00}\rangle$  ( $F_{\text{succ}}$ ) and the probability of success ( $p_{\text{succ}}$ ), for which there is always a trade-off between both variables.

In the following subsections, we describe the main characteristics of the distillation protocols used in this report: (1) BBPSSW, (2) DEJMPS, (3) EPL, and (4) 3-to-1 protocol introduced by D. P. Chi *et al.* [1]. The first three schemes are 2-to-1 protocols, meaning that they consume 2 noisy pairs to obtain another one with higher fidelity.

### A. BBPSSW

According to Bennett *et al.* [4], the BBPSSW protocol can be used to create maximally entangled states  $|\phi_{00}\rangle$  with any desired accuracy from several copies of Werner states, as long as the initial fidelity fulfills  $F > 1/2$ . The implementation of this protocol is described in Figure 1, where the success outcome is given when the measurement results are the same. The expression for the fidelity of success of the BBPSSW

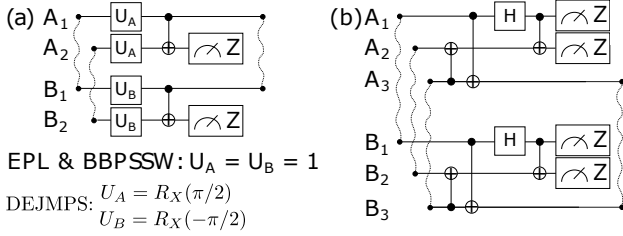


**FIGURE 1:** Implementation of the described protocols into a quantum circuit between Alice ( $A_i$ ) and Bob ( $B_i$ ). The 2-to-1 protocols are sketched in (a) and the 3-to-1 in (b).

protocol (assuming perfect gates) is the following:

$$F_{\text{succ}} = \frac{F^2 + \left(\frac{1-F}{3}\right)^2}{p_{\text{succ}}}, \quad (2)$$

where

$$p_{\text{succ}} = F^2 + 2F\frac{1-F}{3} + 5\left(\frac{1-F}{3}\right)^2, \quad (3)$$

and it fulfills  $F_{\text{succ}} > F$  for  $F > 1/2$ .

However, including the possibility that the gates might be imperfect, the range for which the protocol works ( $F_{\text{succ}} > F$ ) is reduced to  $F \in [F_{\min}, F_{\max}]$ , with

$$F_{\max, \min} = \frac{3}{4} \pm \frac{1}{4} \sqrt{4 + \frac{6}{p} - \frac{9}{p^2}} \quad (4)$$

where  $p$  is the parameter characterising two-qubit operation error (with  $p = 1$  for ideal gates). In this case, the CNOT gate must meet a threshold value of  $p = 92.7\%$  [5].

### B. DEJMPS

The DEJMPS protocol was introduced by Deutsch *et al.* [6] and it is conceptually similar to the BBPSSW protocol. Its implementation is described in Figure 1 and the success outcome is when the measurement results are the same. The main differences with the BBPSSW are that the DEJMPS can also operate on states diagonal in a Bell basis and it has higher efficiency. The expressions for  $F_{\text{succ}}$  and  $p_{\text{succ}}$  can be found in the original paper [6] (assuming perfect gates) and, when applied to the Werner state, they result in the same ones as the BBPSSW. The DEJMPS protocol with ideal gates works only for EPR pair fidelities with  $F > 1/2$ , i.e.  $F_{\text{succ}} \geq F$  if  $F \in [1/2, 1]$ .

When including imperfect gates, the range of  $F$  in which the protocol works is reduced to  $F \in [F_{\min}, F_{\max}]$  with

$$F_{\max, \min} = \frac{3}{4} \pm \frac{1}{4} \sqrt{10 - \frac{9}{p^2}} \quad (5)$$

where  $p$  is the parameter characterising two-qubit operation error, with  $p = 1$  corresponding to ideal gates [7]. In this case, the maximum achievable fidelity is limited by  $F_{\max}$  and the CNOT gate must work with a reliability of at least 95% ( $p = \sqrt{9/10} \approx 0.95$ ).

### C. EPL

As the name suggests, the Extreme Photon Loss Protocol (EPL), which was first proposed in [8], was designed for entanglement generation schemes that use a single photon detection system. The circuit that implements this protocol is shown in Figure 1. The distillation scheme succeeds if the measurement outcome is 11.

It is worth mentioning that this protocol works more efficiently when the input state is an R state [9]. Applying this protocol to two copies of R states, the success fidelity  $F_{\text{succ}} = 1$  is achieved with probability of success  $p_{\text{succ}} = p^2/2$ .

### D. 3-TO-1 PROTOCOL

The 3-to-1 protocol that we consider was proposed by D. P. Chi *et al.* [1], and it is depicted in Figure 1. As opposed to the 2-to-1 protocols described previously, this protocol uses three input Werner states of fidelity  $F$  to obtain a single output state of fidelity  $F_{\text{succ}}$ . The success outcome corresponds when the final measurements satisfy  $A_1 = B_1$  and  $A_2 = B_2$ . The success probability and success fidelity (assuming perfect gates) are given by

$$p_{\text{succ}} = \frac{(1 + 2F)(7 - 14F + 16F^2)}{27}, \quad (6)$$

$$F_{\text{succ}} = \frac{2 - 7F + 14F^2}{7 - 14F + 16F^2}. \quad (7)$$

For input fidelities  $F > 1/2$ , the success fidelity is greater than with the DEJMPS and BBPSSW (see Section VI-A). As a trade-off, we need one more state in the input.

## II. RESEARCH QUESTIONS

In any real device, there are always some imperfections or non-ideal behaviours that lead to different types of errors. The protocols described in the previous section allow to increase the fidelity of the shared EPR pairs, thus they are used to correct the imperfections that may have appeared in the pair initialization. Nevertheless, there are experimental errors related to the performance of the gates used in the protocols that are not taken into account when determining the theoretical  $F_{\text{succ}}$  and  $p_{\text{succ}}$ . In order to better understand how these protocols work in an actual experiment, we need to study their behaviour including also non-ideal gates.

For this reason, our general research question is to get a first characterization of this behaviour by analysing the increase of fidelity  $\Delta F = F_{\text{succ}} - F$  as a function of the input pair and gate fidelities,  $F_{\text{EPR}}$  and  $F_G$  respectively. For answering this question, we will study the following items:

- assessment of the numerical errors to understand the accuracy of the obtained results,
- region in the  $F_G - F_{\text{EPR}}$  plane in which the protocol is useful, i.e. there is an increase of the fidelity ( $\Delta F > 0$ ),
- minimum  $F_G$  needed for the protocol to be useful,
- average of  $\Delta F$  and  $p_{\text{succ}}$  in the region that the protocol is useful (to have an estimate of their performance).

From the results of these research questions, we will be able to get a first general idea of the effect of imperfect

gates in the protocols and to select the best protocol given the output pair fidelity requirements ( $F_{\text{succ}}$ ) and hardware performance (e.g.  $F_G$ ).

### III. METHODOLOGY

In order to evaluate the performance of the four protocols mentioned in Section I, we made use of NetQASM, a low-level instruction set architecture for quantum internet applications, and its software development kit (SDK) in Python [10]. The SDK was exploited by means of a backend quantum simulator NetSquid, that allowed us to run the distillation protocols subjected to depolarizing noise. The depolarizing channels used for the imperfect EPR pair initialization and non-ideal gates are characterised by  $p_G$  and  $p_{\text{EPR}}$  respectively (corresponding to  $p$  from Equation (1)).

The approach adopted to analyze our research questions has two parts: (1) an initial characterisation to narrow the studied region of the  $F_G - F_{\text{EPR}}$  plane, and (2) a deeper analysis of the protocols through our research questions. In the first part, we inspect the execution of each protocol in the whole range of possible values for  $F_G \in [0, 1]$  and  $p_{\text{EPR}} \in [0, 1]$  by considering 10 equally spaced points for both parameters. From the gathered data, we can narrow the range of  $F_G$  and  $F_{\text{EPR}}$  to the region in which  $\Delta F > 0$ , as well as select the optimal number of simulations  $N_{\text{sim}}$  to perform for each pair of  $\{F_G, F_{\text{EPR}}\}$ .

In the second part, we use the narrower range of  $F_G$  and  $F_{\text{EPR}}$  to calculate  $F_{\text{succ}}$  and  $p_{\text{succ}}$ , as well as an assessment of the numerical errors. From the plots  $F_{\text{succ}}(F_G, F_{\text{EPR}})$  and  $p_{\text{succ}}(F_G, F_{\text{EPR}})$ , we can discuss our research questions.

### IV. RESULTS

This section contains the complete comparison between the protocols for each point enumerated in the research question section (each one discussed in a different section). The analysis of the  $F_G - F_{\text{EPR}}$  range is done in Section VI-C, which results in the narrower ranges:  $F_G \in [0.8, 1]$  and  $F_{\text{EPR}} \in [0.65, 1]$ . The selected number of simulations for each point  $\{F_G, F_{\text{EPR}}\}$  is  $N_{\text{sim}} = 200$  because we did not observe a significant decrease in the numerical error upon increasing  $N_{\text{sim}}$  (complete discussion in Section VI-D).

#### A. ASSESSMENT OF NUMERICAL ERRORS

The aim of assessing the numerical errors is to understand the accuracy of the simulations in order to correctly discuss the obtained results for the research questions.

We have calculated the errors of  $F_{\text{succ}}$  for the BBPSSW, DEJMPS and 3-to-1 protocols using the formulas from Section I and the simulation's results with  $F_G = 1$ , see Figure 2. Their average values and the average standard deviation from the simulations ( $\sigma_F$ ), are summarized in Table 1 (the formulas that we used are described in its caption). For the  $\sigma_F$  of the EPL protocol, see Section VI-B.

Noteworthy, the standard deviation is in general larger than the absolute error but, upon averaging, they are similar. Then, as we cannot evaluate the errors when  $F_G < 1$  for all

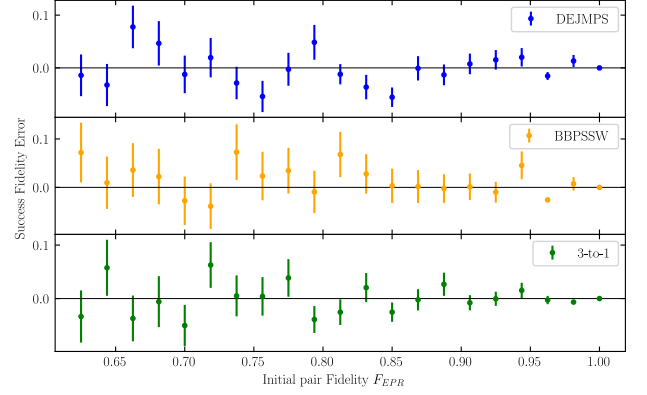


**FIGURE 2:** Representation of the errors for  $F_G = 1$  (corresponding to  $F_{\text{succ}}(\text{theoretical}) - F_{\text{succ}}(\text{sim})$ ) and the  $\sigma_F$  of the numerical simulations.

**TABLE 1:** Average errors (absolute and relative) and standard deviations ( $\sigma_F$  and relative) of  $F_{\text{succ}}$  when  $F_G = 1$ . The averaging is done using the points  $F_{\text{EPR}} \in [0.65, 1]$ . The standard deviation  $\sigma_F$  is calculated using the  $F_{\text{succ}}$  from the simulations that had a successful distillation. The relative  $\sigma_F$  is calculated as  $\sigma_F$  divided by the average of  $F_{\text{succ}}$ .

Protocol	abs. error	$\sigma_F$	rel. error [%]	rel. $\sigma_F$ [%]
BBPSSW	0.026	0.038	3.3	5.0
DEJMPS	0.025	0.026	3.2	3.3
3-to-1	0.022	0.027	2.7	3.3

protocols, we may assume that the actual value of  $F_{\text{succ}}$  is between  $F_{\text{succ}}(\text{sim}) \pm \sigma_F$ . In fact, this assumption holds for the BBPSSW and DEJMPS, which has been checked using the expression for  $F_{\text{succ}}$  when  $F_G < 1$  from [5] and [7] (obtaining a maximum error of 15% and 17% respectively).

Another important characteristic, is that the standard deviation depends on the initial pair fidelity  $F_{\text{EPR}}$ . In particular,  $\sigma_F$  gets lower when increasing  $F_{\text{EPR}}$ , because the fidelity outcome of the simulations is mainly  $F_{\text{succ}} = 1$  when  $F_{\text{EPR}} \rightarrow 1$ . Such dependence will be important when determining the  $\Delta F > 0$  region in the next section.

#### B. DETERMINATION OF THE $\Delta F > 0$ REGION

The region of the  $F_{\text{EPR}} - F_G$  plane in which  $\Delta F > 0$  (named " $\Delta F > 0$  region") is key to determine under which conditions the protocols are useful. For the determination of this region, we have considered three different cases regarding the accuracy of the results discussed in the previous section:

- 1) Great certainty that  $\Delta F > 0 \Rightarrow \Delta F > \sigma_F$
- 2) Unsure whether  $\Delta F > 0$  or  $\Delta F < 0 \Rightarrow -\sigma_F < \Delta F < \sigma_F$
- 3) Great certainty that  $\Delta F < 0 \Rightarrow \Delta F < -\sigma_F$

where it has to be taken into account that  $\sigma_F$  depends on  $F_{\text{EPR}}$  and  $F_G$ . For each protocol, these three cases are plotted in Figures 3 and 4 (see Section VI-E for  $\Delta F(F_{\text{EPR}}, F_G)$  plots). The areas of the  $\Delta F > \sigma_F$  case are reported in Table 2.

The two protocols with larger area for case 2 (unsure situation) correspond to BBPSSW and EPL. This can be explained by the fact that they use a low number of gates and therefore we expect  $\Delta F$  to decrease slowly when  $F_G$

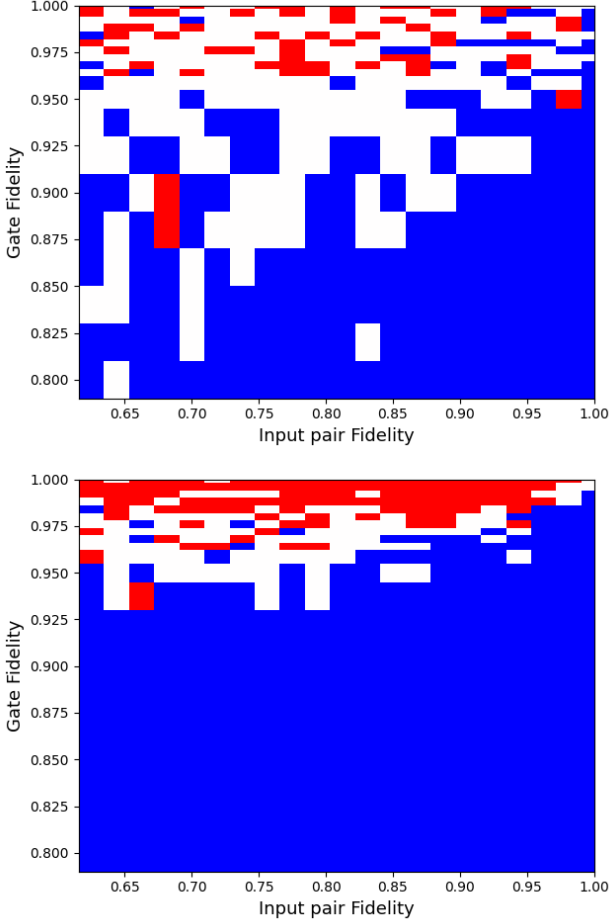


**FIGURE 3:** Representation of the three cases described in Section IV-B in the plane  $F_{\text{EPR}} - F_G$  for the EPL (top) and 3-to-1 (bottom) protocols. Color blue represents  $\Delta F < -\sigma_F$ , white  $-\sigma_F < \Delta F < \sigma_F$ , and red  $\Delta F > \sigma_F$ .

decreases, which creates a larger region where  $\Delta F_{\text{sim}} \approx 0$  and we are unsure whether  $\Delta F_{\text{theo}} > 0$  or  $\Delta F_{\text{theo}} < 0$ .

### C. MINIMUM GATE FIDELITY NEEDED FOR $\Delta F > 0$

Now that we know the exact region of optimal operation of the four protocols, we can extract some parameters that characterize them. From Figures 3 and 4, we can extract the minimum gate fidelity for which we consistently obtain an increase  $\Delta F > \sigma_F$  (reported in Table 2).

On the one hand, it is expected that the protocols BBPSSW and EPL have the lowest minimum gate fidelity, since they use the least number of gates. Moreover, despite using more gates, the protocol 3-to-1 has a lower minimum gate fidelity than DEJMPS, due to the fact that it has a higher increase in fidelity (see Section VI-A), thus its region for  $\Delta F > \sigma_F$  starts sooner. From the theoretical formulas for  $F_{\text{succ}}$  when  $F_G < 1$  reported in [5] and [7], the theoretical minimum  $F_G$  for DEJMPS and BBPSSW are 0.981 and 0.972 respectively, which match our results within the uncertainty  $\sigma_F$ .

On the other hand, regarding the areas of the  $\Delta F > \sigma_F$  region (A), the BBPSSW and DEJMPS protocols have similar

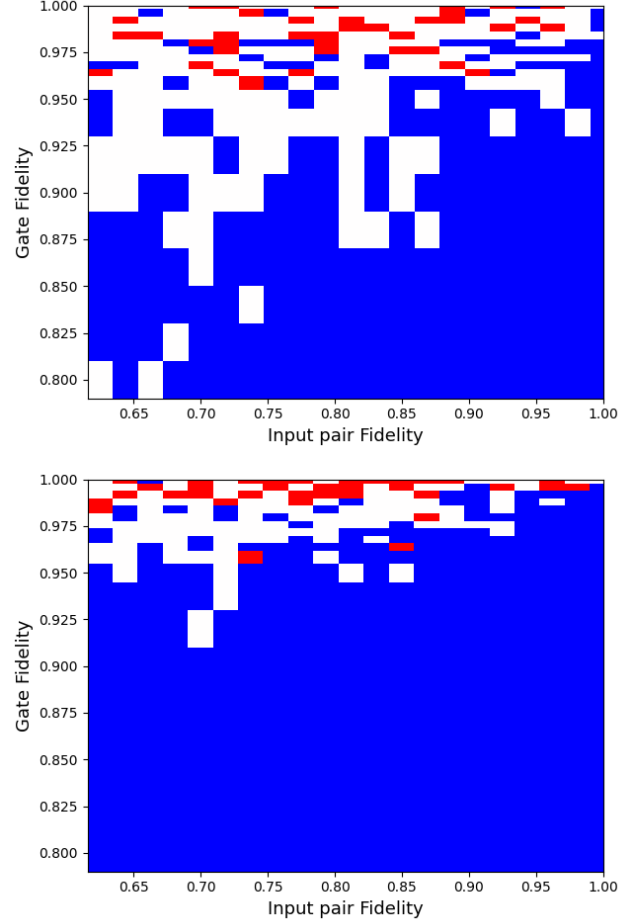


**FIGURE 4:** Representation of the three cases described in Section IV-B in the plane  $F_{\text{EPR}} - F_G$  for the BBPSSW (top) and DEJMPS (bottom) protocols. Color blue represents  $\Delta F < -\sigma_F$ , white  $-\sigma_F < \Delta F < \sigma_F$ , and red  $\Delta F > \sigma_F$ .

values because they have the same expressions for  $F_{\text{succ}}$  and  $p_{\text{succ}}$ , with  $A_{\text{BBPSSW}} > A_{\text{DEJMPS}}$  because the latter uses more gates and thus the increase of fidelity decreases with lower  $F_G$ . The 3-to-1 protocol has the largest area due to the fact of being the protocol with highest theoretical  $\Delta F$  and thus with more probability that  $\Delta F > \sigma_F$ .

### D. AVERAGE $p_{\text{succ}}$ AND $\Delta F$ IN THE $\Delta F > 0$ REGION

The performance of the four protocols has been compared by means of the average of  $p_{\text{succ}}$ ,  $F_{\text{succ}}$  and  $\Delta F$  over the region of case 1 ( $\Delta F > \sigma_F$ ). The corresponding results are displayed in Table 2. Regarding the average increase of fidelity  $\langle \Delta F \rangle$ , the BBPSSW, DEJMPS and 3-to-1 protocols have similar values around  $\langle \Delta F \rangle \approx 0.06$  and the EPL protocol has a higher value, i.e.  $\langle \Delta F \rangle \approx 0.09$ . Regarding the  $\langle p_{\text{succ}} \rangle$ , a clear trade-off between  $p_{\text{succ}}$  and  $F_{\text{succ}}$  is present, which is in agreement with the theoretical framework. In particular, the EPL protocol has the highest increase of fidelity but its probability of success is the lowest one.

It is worth noticing that the values shown for  $\langle F_{\text{succ}} \rangle$  are higher with respect to the theoretical values. This is due to the

**TABLE 2:** Average success results for  $p_{\text{succ}}$ ,  $F_{\text{succ}}$  and positive increase in fidelity after the entanglement distillation when they show a  $\Delta F > 0$ . The average of variable  $X$  in the points where  $\Delta F > 0$  is represented as  $\langle X \rangle$ . The area corresponds to the surface where  $\Delta F > \sigma_F$  and it is measured in arbitrary units.

Protocol	min. $F_G$	$\langle p_{\text{succ}} \rangle$	$\langle F_{\text{succ}} \rangle$	$\langle \Delta F \rangle$	Area
BBPSSW	0.96	0.76	0.86	0.06	0.09
DEJMPS	0.98	0.75	0.84	0.05	0.08
3-to-1	0.97	0.56	0.86	0.07	0.24
EPL	0.96	0.38	0.89	0.09	0.14

fact that for the computation of this data, we only took into account the points of the simulation for which  $\Delta F > \sigma_F$ . We discarded for instance those that theoretically had  $\Delta F_{\text{theo}} \gtrsim \sigma_F$  (low increase), but due to negative numerical errors, i.e.  $F_{\text{sim}} - F_{\text{theo}} < 0$ , they finally show  $\Delta F_{\text{sim}} < \sigma_F$ . However, we keep the points that have a positive numerical error, i.e.  $\Delta F_{\text{sim}} > \Delta F_{\text{theo}} > \sigma_F$ , resulting in an overestimation of  $\langle F_{\text{succ}} \rangle$  and  $\langle \Delta F \rangle$ . Nevertheless, as this overestimation appears equally in all the four protocols under investigation, the comparison between the output values in each protocol is still valid and meaningful to address our research questions (but the results cannot be used as absolute values). Noteworthy, the discrepancy in relation to the real values gets smaller with increasing number of simulations as  $\sigma_F \rightarrow 0$ .

### E. GENERAL PROTOCOL SELECTION

After completing the characterization of the four protocols through the research questions, we can build a general recipe about which protocol to use given a list of requirements, including the desired increase of fidelity, hardware gate fidelity ( $F_G$ ), number of attempts ( $N$ ), and range of initial pair fidelity ( $F_{\text{EPR}}$ ). The minimum conditions where each protocol performs correctly and the expected increase of fidelity are:

- **EPL.**  $F_G \geq 0.96$  and high  $N$  (low  $p_{\text{succ}}$ )  $\Rightarrow$  high increase of fidelity
- **BBPSSW.**  $F_G \geq 0.96$ , low  $N$  (high  $p_{\text{succ}}$ ) and  $F_{\text{EPR}} \in [0.7, 0.9] \Rightarrow$  medium increase of fidelity
- **DEJMPS.**  $F_G \geq 0.98$  and low  $N$  (high  $p_{\text{succ}}$ )  $\Rightarrow$  medium increase of fidelity
- **3-to-1.**  $F_G \geq 0.97$ , moderate  $N$  (medium  $p_{\text{succ}}$ ) and be able to store 3 EPR pairs  $\Rightarrow$  medium increase of fidelity

### V. CONCLUSIONS

In this report, we have simulated the effect of 4 distillation protocols (namely BBPSSW, DEJMPS, EPL and 3-to-1) on Werner states without assuming ideal gates. We have shown that it is possible to achieve an increase of the pair fidelity if the gate fidelity is higher than approximately 0.96. Moreover, including the success probability results, we have built a general recipe for selecting the best protocol given a list of requirements.

Despite doing an analysis of the numerical errors for a more accurate discussion of the results, we also need to take into account the limitations of the model used. Even though

the measurements are not taken to have errors, they could be a concern in a real implementation. For instance, the 3-to-1 protocol might perform worse since it has a higher number of measurements compared to the other protocols. In addition, we have assumed that we start with a Werner state, which might not be natural to some specific implementations of the hardware and thus the obtained results could vary.

Even though the model has limitations, it is useful for having a clearer picture of how entanglement distillation protocols succeed in generating a better entangled pair under specific conditions, i.e. imperfect gates. For real application and implementation of these protocols on a hardware device, high gate fidelities are needed in order for the distillation protocols to be useful, thus the cost-benefit analysis for the exploitation of entanglement distillation is definitely a factor to be taken into account.

We conclude this report by highlighting the advisable future work of entanglement distillation regarding the specific case of this study. As reported in I-C, the EPL protocol works well for R states, but no relevant information is present in the literature about the performance of this protocol with Werner states. For this reason, the development of a theoretical model for EPL protocol that includes the expected values of  $F_{\text{succ}}$  and  $p_{\text{succ}}$  for both ideal and non-ideal gates could help get error estimates and clearer comparisons between protocols. In addition, increasing the number of simulations will reduce the numerical error and allow to obtain more accurate results. Moreover, to achieve a more realistic behaviour of the entanglement distillation protocols, a measurement error model could be added to the simulations. Finally, as the pair fidelity requirements is usually given by a minimum threshold, it would be also interesting to characterize the behaviour of the protocols after a certain number of iterations.

### REFERENCES

- [1] D. P. Chi, T. Kim, and S. Lee, "Efficient three-to-one entanglement purification protocol," *Physics Letters A*, vol. 376, no. 3, pp. 143–146, 2012.
- [2] M. A. Nielsen and I. L. Chuang, "Quantum computation and quantum information," *Phys. Today*, vol. 54, no. 2, 2001.
- [3] C. King, "The capacity of the quantum depolarizing channel," *IEEE Transactions on Information Theory*, vol. 49, no. 1, pp. 221–229, 2003.
- [4] C. H. Bennett, G. Brassard, S. Popescu, B. Schumacher, J. A. Smolin, and W. K. Wootters, "Purification of noisy entanglement and faithful teleportation via noisy channels," *Physical Review Letters*, vol. 76, no. 5, p. 722, 1996.
- [5] W. Dür and H. J. Briegel, "Entanglement purification and quantum error correction," *Reports on Progress in Physics*, vol. 70, no. 8, p. 1381, 2007.
- [6] D. Deutsch, A. Ekert, R. Jozsa, C. Macchiavello, S. Popescu, and A. Sanpera, "Quantum privacy amplification and the security of quantum cryptography over noisy channels," *Physical review letters*, vol. 77, no. 13, p. 2818, 1996.
- [7] W. Dür, H.-J. Briegel, J. I. Cirac, and P. Zoller, "Quantum repeaters based on entanglement purification," *Physical Review A*, vol. 59, no. 1, p. 169, 1999.
- [8] C. H. Bennett, D. P. DiVincenzo, J. A. Smolin, and W. K. Wootters, "Mixed state entanglement and quantum error correction," *Physical Review A*, vol. 54, no. 5, 1996.
- [9] F. Rozpedek, "Building blocks of quantum repeater networks," 2019.
- [10] A. Dahlberg, B. van der Vecht, C. D. Donne, M. Skrzypczyk, I. te Raa, W. Kozłowski, and S. Wehner, "Netqasm - a low-level instruction set architecture for hybrid quantum-classical programs in a quantum internet," p. 1, 2021.



## VI. SUPPLEMENTARY INFORMATION

### A. THEORETICAL CURVES OF $F_{\text{succ}}$ WITH $F_G=1$

In Figure 5 we plot the theoretical curves for the success fidelity as a function of the input pair fidelity (for gate fidelity  $F_G = 1$ ) using Equations (2) and (7).

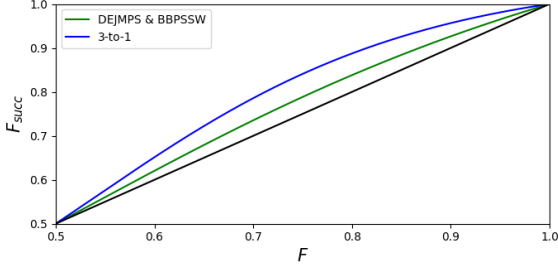


**FIGURE 5:** Theoretical  $F_{\text{succ}}$  as a function of  $F_{\text{EPR}}$  with  $F_G = 1$  for the protocols BBPSSW, DEJMPS and 3-to-1. The black line corresponds to a straight line with slope 1 and crossing the origin.

### B. VALUES AND STANDARD DEVIATION OF $F_{\text{succ}}$ AND $p_{\text{succ}}$ FOR EPL PROTOCOL

The EPL protocol lacks a theoretical framework for the expected values of  $F_{\text{succ}}$  and  $p_{\text{succ}}$ , therefore it is not possible to calculate the numerical error. Nevertheless, the average standard deviation of  $F_{\text{succ}}$  for  $F_G = 1$  is reported in Figure 6.

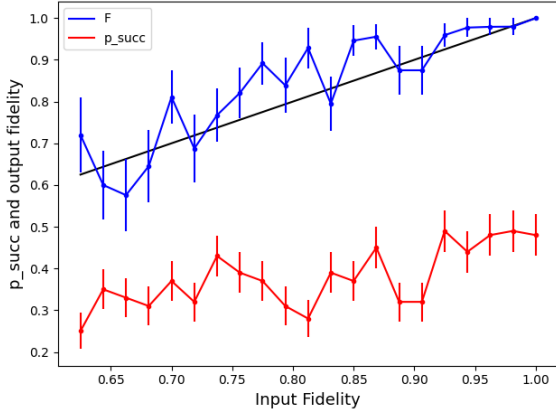


**FIGURE 6:** Representation of  $F_{\text{succ}}$  (blue) and  $p_{\text{succ}}$  (red) and their standard deviation for the EPL protocol.

### C. ANALYSIS OF THE $F_G$ AND $F_{\text{EPR}}$ RANGES

The first (coarse) mesh used to get a first idea of the increase of the fidelity is described by  $F_G^{(i)} = 0.1 \cdot i$  for  $i = 0, 1, \dots, 10$  and  $p_{\text{EPR}}^{(j)} = 0.1 \cdot j$  for  $j = 0, 1, \dots, 10$ , where  $p_{\text{EPR}}$  is the probability that the Werner state is in the  $|\phi_{00}\rangle$  state. This probability is related to the fidelity of the pair by  $F_{\text{EPR}} = (3p_{\text{EPR}} + 1)/4$ .

The results are plotted in Figure 7. The only regions in which there is an increase of the fidelity ( $\Delta F > 0$ ) correspond to  $p_{\text{EPR}} < 0.2$  (which means  $F_{\text{EPR}} < 0.4$ ) and  $F_G$  very close to 1. According to the theoretical formulas, the protocols only have an increase in fidelity  $\Delta F > 0$  for

$F_{\text{EPR}} > 0.5$ . However, the theoretical increase at  $F_{\text{EPR}} = 0.5$  is  $\Delta F = 0$ . Therefore, none of the protocols are useful for  $F_{\text{EPR}} = 0.5$ . From Figure 7, the protocols start to have an increase in fidelity for  $p_{\text{EPR}} > 0.5$  (which means  $F_{\text{EPR}} > 0.625$ ).

Out of the four protocols, the EPL shows the increase of the fidelity for the lowest  $F_G$ , which corresponds to  $F_G \approx 0.85$ . Therefore, the region of the  $F_G - F_{\text{EPR}}$  for the second part described in the methodology (Section III) is  $F_G \in [0.8, 1]$  and  $F_{\text{EPR}} \in [0.65, 1]$ .

### D. ANALYSIS OF THE NUMBER OF SIMULATIONS

In order to know the dependence of the numerical error and number of simulations, we have analysed the DEJMPS protocol when the gate fidelity is fixed at 1, because then it is possible to compare the obtained results of  $F_{\text{succ}}$  and  $p_{\text{succ}}$  with their respective theoretical values. This comparison for  $F_{\text{succ}}$  is included in Figure 8, which shows the expected trend that increasing the number of simulations reduces the numerical error. In particular, there is not difference when using 200 and 400 simulations, therefore the best option is to do 200 simulations for each point, which has an average of 1.3% difference with the theoretical values. Similar results were also obtained for the probability of success, which have not been included.

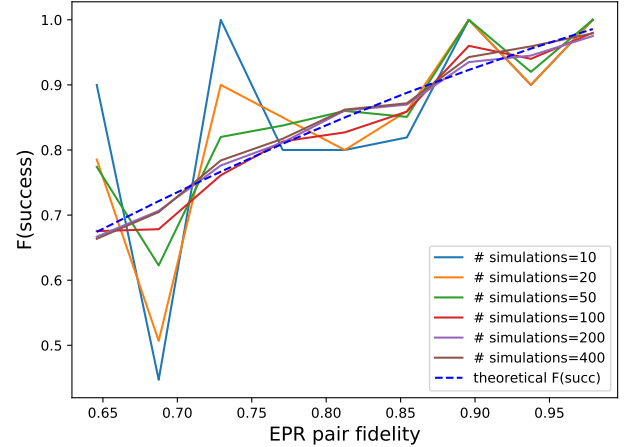


**FIGURE 8:** Success fidelity of the DEJMPS protocol as a function of different input EPR pair fidelity with perfect gates, for different number of simulations used to determine each point.

### E. INCREASE OF FIDELITY AS FUNCTION OF $F_G$ , $F_{\text{EPR}}$

We study the increase in fidelity in the region where our protocols are potentially useful, that is,  $F_G \in [0.8, 1]$  and  $F_{\text{EPR}} \in [0.65, 1]$ , which we determined in Section VI-C. After refining the mesh of gate fidelities and EPR fidelities that we simulate, the increase of fidelity as function of  $F_G$  and  $F_{\text{EPR}}$  for each of the protocols is plotted in Figure 9. Starting from these figures, in Subsection IV-B we carry out an analysis of what region has an actual increase in fidelity, taking into account the standard deviations of the simulations.

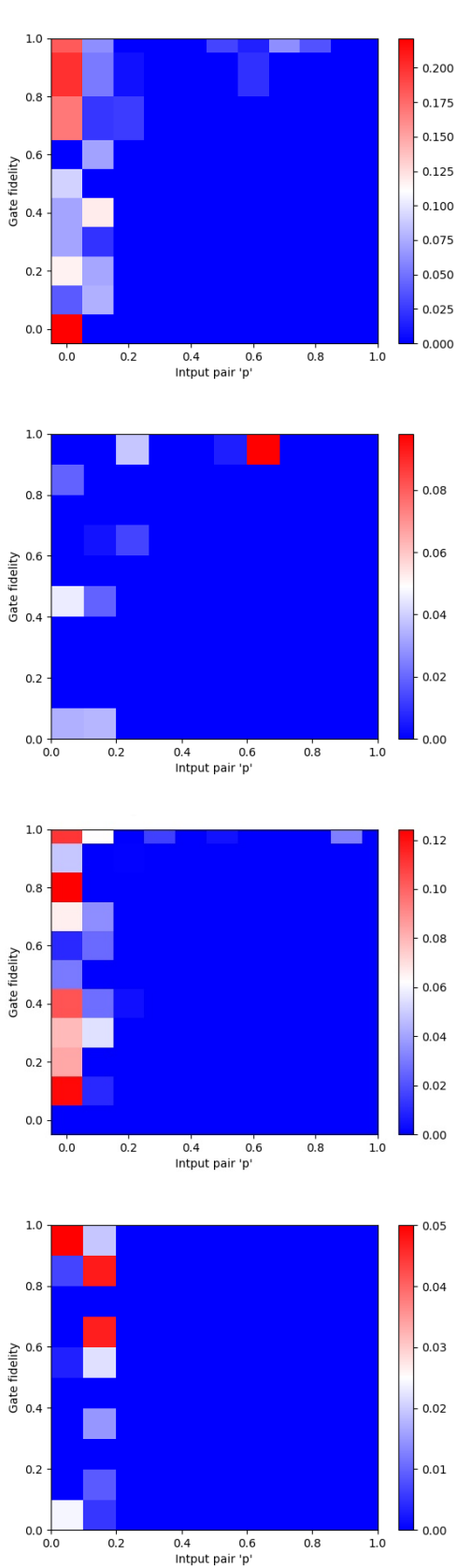


**FIGURE 7:** Representation of  $\Delta F$  in the plane  $F_{\text{EPR}} - F_G$  for EPL, 3-to-1, BBPSSW and DEJMPS (top to bottom) protocols. The points where  $\Delta F < 0$  have been replaced by  $\Delta F = 0$  in order to highlight the regions where  $\Delta F > 0$ .

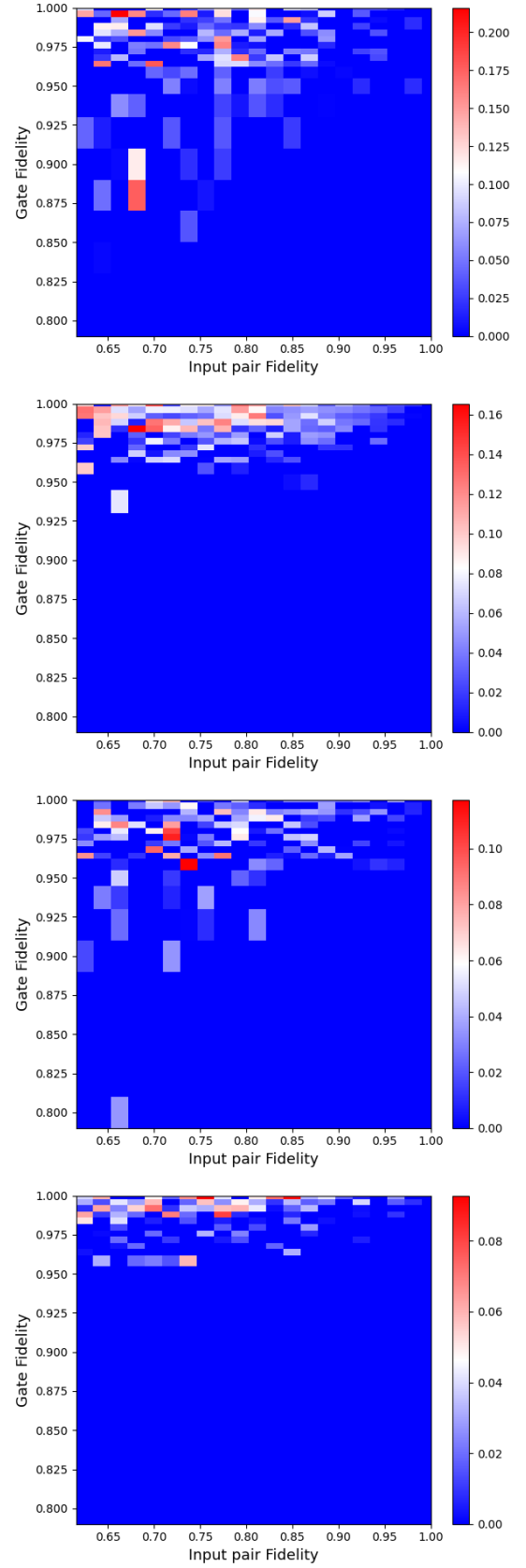


**FIGURE 9:** Representation of  $\Delta F$  in the plane  $F_{\text{EPR}} - F_G$  for the EPL, 3-to-1, BBPSSW and DEJMPS (top to bottom) protocols. The points where  $\Delta F < 0$  have been replaced by  $\Delta F = 0$  in order to highlight the regions where  $\Delta F > 0$ .